Modelling of uncertainties of an emission concentration measurement in stacks

S. Knotek, J. Geršl,

Czech Metrology Institute, Brno, Czech Republic
E-mail (corresponding author): sknotek@cmi.cz

Abstract

This contribution describes a research of measurement uncertainty of industrial emissions flowing through vertical stacks and its dependence on different geometrical configurations and physical conditions. Since the legislative requirements for emission limits from industrial processes are decreasing, the higher measurement accuracy is becoming more important and new uncertainty standards needs to be implemented. This contribution is a part of the research project 18NRM04 Heroes under European Metrology Program for Innovation and Research (EMPIR).
CFD modelling is used to analyse particle distributions in stacks with three different geometries of a supply pipe, different size of the particles and several concentrations. Vertical stack with a circular cross section of a diameter of 0.75 m is considered with the supply pipe containing none, one or two bends. The number of particles entering the stack defines the initial volumetric concentration from 0.1 to 10 mg·m^{-3} with the particle size from 10 to 50 μm.
Concentration fields in several cross-sections were compared and the particle distributions were analysed as functions of the physical conditions and the chosen geometry of the stack. The results show not very high sensitivity of the concentration profiles on the initial concentrations. On the other hand, significant changes of the concentration fields are observed when the stack geometry or the particle diameter is changed. This should be taken into account in the iso-kinetic sampling practise where the overall concentrations are calculated from measurements in several points.

1. Introduction

Several research projects in previous years focused on emission measurements in industrial stacks and a lot of effort was given to uncertainty evaluation of the corresponding measurement techniques (see e.g. the IMPRESS and IMPRESS II projects within the EMRP and EMPIR research programs for metrology). The presented research is a part of the EMPIR project 18NRM04 HEROES (Determining new uncertainty requirements for increasingly stringent legislative HCL industrial emission limits). Since the HCL Standard Reference Method (SRM, EN 1911) [1] is unable to fulfill the uncertainty requirements in Best Available Techniques (BAT) [2] [8], one specific objective of the project is to contribute to a revision of EN 1911 by data, methods or recommendations necessary for the new uncertainty requirements. The aim of this paper is to check if the current measurements standards, e.g. EN 15259:2007 [3] defining the sampling points for the SRMs, are sufficient for real stack configurations where complicated flow fields can be established. For this purpose, the previous research of flow rate measurement [3, 4] is followed by this work which focuses on particle distributions in stacks and the related concentration measurement uncertainties.

2. Methods

In order to investigate the particle distributions in stack and their dependence on different geometrical and physical conditions, the numerical methods of Computational Fluid Dynamic (CFD) were chosen. The simulations were performed by OpenFOAM-5.x, free open-source software. In the next sections the settings of testing cases and solvers will be described.

2.1 Geometrical design of testing stack simulator

In order to investigate how the emission measurements can be influenced by geometrical arrangement, three basic geometrical configurations, which can occur in real stack system, were used. The studied stack consists from straight vertical part along z-axis, T-junction with blind bottom and three different supply pipes entering into vertical stack pipe in direction of x-axis. In Figure 1, the straight supply pipe, a), single 90° elbow, b), and double 90° elbows c) are depicted. Note, that these topologies are similar as used in paper [4] and [5], where simulated velocity fields were used for discussion of uncertainty of flow rate measurements with Pitot tube or ultrasonic flow measurement. The diameter D equals 0.75 m, since the computational cost for original diameter 1.5 m as used in [4] and [5] has been shown as too high for finishing all defined combinations of parameters in reasonable time frame.

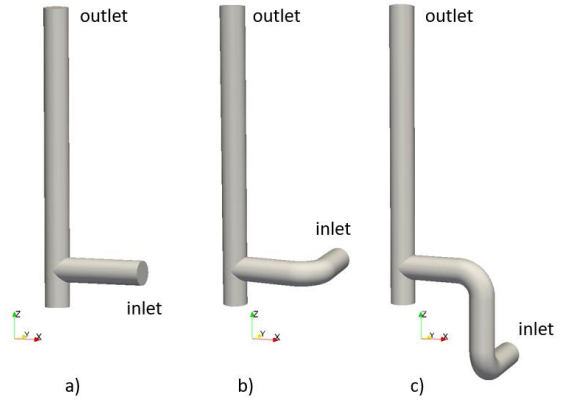

Figure 1: Geometrical configuration of stacks. a) straight supply pipe b) the supply pipe with single 90° elbow and c) the supply pipe with double 90° elbows.

2.2 Mesh

In purpose of CFD simulations, the structured meshes were prepared using *blockMesh* tool implemented in OpenFOAM. Taking into account the bulk velocity U_b=5 m/s, the grids were designed so that dimensionless first wall cell thickness y+ equals 30 and free stream dimensionless cell size z+ equals 300. With this refinement, the number of cells range from 1.5 million for straight pipe supply case to 2.2 million for double elbow supply pipe case. The detail of the mesh refinement in T-junction is depicted in Figure 2.

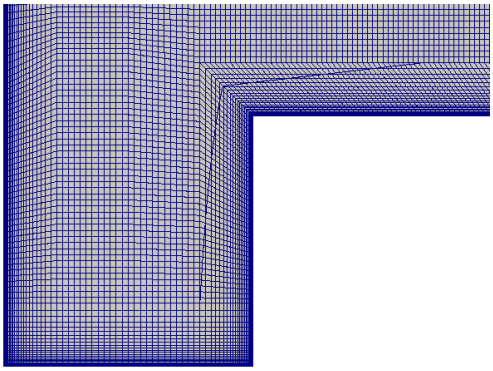

Figure 2: Mesh density in the cross-section of the T-junction.

2.3 Numerical setting and boundary conditions

For resolving the flow of particles, so called Eulerian-Lagrangian approach was used. In this attitude, the fluid flow is simulated based on Euler approach, i.e. by resolving of flow velocity field using Reynolds averaged Navier-Stokes equations in connection with appropriate turbulence model and the particles flow is resolved using Lagrangian Particle Tracking (LPT) approach.

For coupled resolution of both approaches, the *MPPICFoam* (Multi-Phase Particle In Cell, see [6]) solver implemented in OpenFOAM was used.

Since the concentration of emission particles are supposed to be relatively low, only so-called one-way coupling was used for resolution of particle transport inside stack and influence of particle on fluid (two-way coupling) as well as particle interaction (four-way coupling) are neglected. In this case the trajectories of each particle, x_p, is given as

$$\frac{dx_p}{dt} = u_p \tag{1}$$

where particle velocity u_p is given by formula

$$m_p \frac{du_p}{dt} = F_p, \tag{2}$$

where m_p is weight of particle and F_p sum of forces acting on spherical particle, see [6] for details.

For solution, the default combination of first and second order numerical schemes were adopted. The boundary conditions of fluid flow were defined according to classical scheme of velocity inlet and pressure outlet, i.e. a constant uniform velocity profile was defined at the inlet and constant zero pressure was prescribed at the outlet plane on top of the vertical stack. On the walls, the no-slip velocity condition was set using zero velocity and zero normal pressure gradient. The turbulent kinetic energy, *k*, and the rate of dissipation of turbulent kinetic energy, ε, were set at the inlet by values related to 5% turbulence intensity. The default wall functions have been used ion the walls.

2.4 Physical properties

The fluid medium was supposed to have kinematic viscosity $1.5{\cdot}10^{-5}$ m^2/s and density 1.2 kg/m^3. The emission particles were modeled as spherical particles with diameter from 10 to 50 μm and density 2300 kg/m^3. The volumetric concentration was modeled from 0.1 to 10 mg/m^3.

3. Results and discussion

3.1. Resulting velocity fields

The velocity fields computed by *MPPICFoam* was observed to be identical as given by *simpleFoam* in [5], what is however in correspondence with the assumption that the particles are not influencing the fluid flow and that both solvers are consistent in resolution of basic fluid flow.

In Figure 3, the velocity vector fields in horizontal (parallel to x-y plane) cross-sections in distance 5D downstream from T-junction are depicted for all three geometries. The swirl structures are generated for all three cases. Two counter-rotating swirls are observed for straight supply pipe, while single clockwise and counter-clockwise swirl is depicted for single elbow and double elbow pipe supply, respectively. Note, that as can be seen from colors, the highest velocities are observed for

double elbow supply pipe, so the swirl can be assessed as the strongest from all three cases.

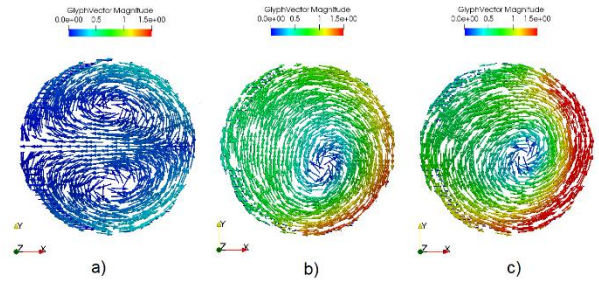

Figure 3: The swirl structures in stack depicted at horizontal cross-section in distance 5D downstream from T-junction: a) two swirls for straight supply pipe, b) one clockwise swirl for single elbow supply pipe and c) one counter clockwise swirl for double elbow supply pipe.

In Figure 4, the distribution of axial velocity components in horizontal cuts along the stacks are depicted at 2, 3, 4, 5, 6 and 7 diameters from T-junction. The (x, y) location of the minimal and maximal axial velocity remains in the symmetry plane of the straight supply pipe for all distances, while clockwise and counter-clockwise movement is observed for single elbow and double elbow supply pipe, respectively. The angular positions of the maximal axial velocity as a function of distance from T-junction can be found in [4]. As can be seen from maximal and minimal values depicted by color map, the extremal values are decreasing along the distance from T-junction as the velocity profiles are developed and becomes flatter.

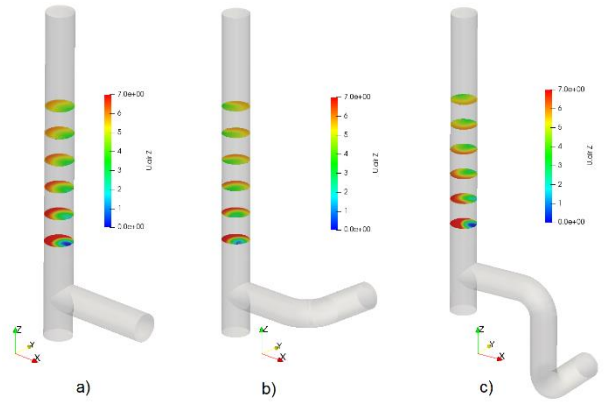

Figure 4: Distribution of axial velocity component in horizontal cuts along the stack.

3.2 Resulting concentration field

In this section, the way in which the velocity distributions and characteristics are influencing the distribution of emission particles is discussed.

As mentioned above, the *MPPICFoam* solver used for simulation is transient, so time particle flow in time interval of 15 seconds was computed for each test case. It was observed that after about 10 seconds, the concentrations fields do not change significantly, although the number of particles in domain is still increasing as some particles are remaining in T-junction and in wall vicinity as is discussed in next paragraph. Regarding the facts just outlined, note that the particle distribution figures depicted bellow were realized from sampling time 10 seconds after beginning of simulation.

For the global view, the comparison of particle distributions for particle diameters of 10, 20 and 50 μm is depicted in Figures 5, 6 and 7 for all three geometries at plane section y=0. Note, that the particles visible in the figures are given not by pure section y=0, but by projection of all particles located in the domain which y coordinates are in certain time in range from y=-0.003 m to y=0.003 m.

It is observed that the particle diameter has significant influence on the concentration field. The increasing diameter leads to stronger deposition of particles on walls, while decreasing diameter support better mixing of particles and the distribution is more homogenized. Although the simulated results show clear dependency just described, it has to be noted that the simulation of particles near the wall is still challenging task for CFD modelling and special models are under development to include isotropic turbulence. Special models as Continuous Random Walk models, see e.g. [7], could be used for better simulation of near wall particle concentration. However, just for the purpose of concentration evaluation in sampling points according to standard [3], the near wall distribution is not decisive since the sampling points are nevertheless not located in the wall vicinity.

The Figures 5-7 also show the influence of the geometry. In the straight pipe supply, cases a), the particles are at primary accumulated on the opposite wall to supply pipe and secondary spread out along the walls. With increasing distance from T-junction, see Figure 8, the particles are distributed more symmetrically according axial axis. In case of the single elbow supply pipe, cases b) in Figure 5-7, the influence of swirl is clearly visible. Figure 8 support the imagination how the particles are moving along the axial axis in dependence on the clockwise swirl. Finally, the movement of particles in double elbow supply pipe cases c) in Figure 5-7 is influenced by counter-clockwise rotating swirl, however due to more difficult velocity filed, the particles are more uniformly distributed in comparison to previous two configurations. Strong uniform distribution is visible also from Figure 7 where locations of particles of diameter 10 μm are depicted.

The results just outlined are in agreement with well-known observations that big particles in bend suffer from strong deposition while smaller and lighter particles are following more easily the basic flow stream and even more decreased weight causes distribution influenced by turbulence perturbations.

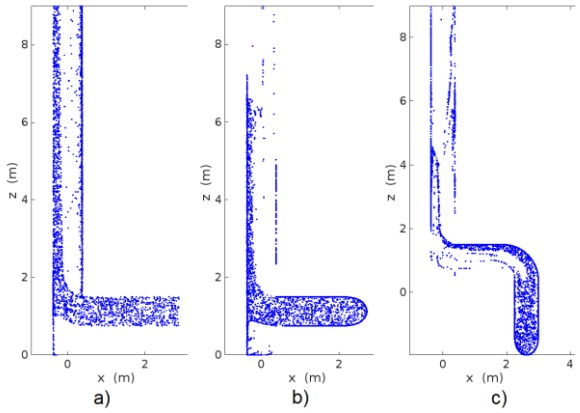

Figure 5: Particles distribution in vertical cut y=0 for inlet concentration 10 mg/m^3 and particle diameter 50 µm for a) straight supply pipe, b) single elbow supply pipe, c) double elbow supply pipe.

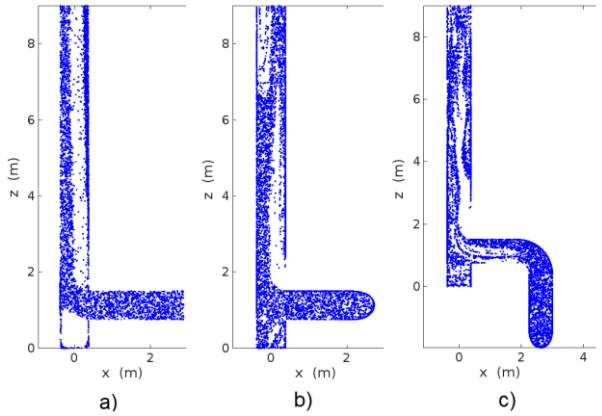

Figure 6: Particles distribution in vertical cut y=0 for inlet concentration 1 mg/m^3 and particle diameter 20 µm for a) straight supply pipe, b) single elbow supply pipe, c) double elbow supply pipe.

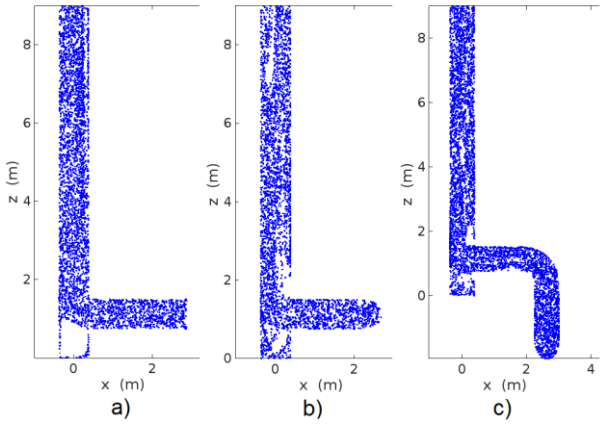

Figure 7: Particles distribution in vertical cut y=0 for inlet concentration 0.1 mg/m^3 and particle diameter 10 µm for a) straight supply pipe, b) single elbow supply pipe, c) double elbow supply pipe.

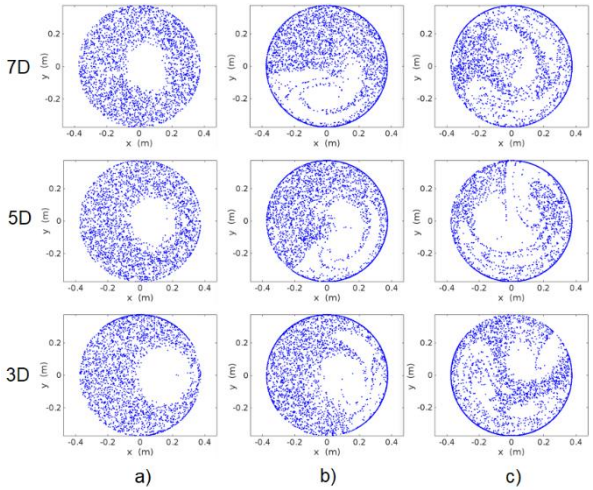

Figure 8: Particle distribution in horizontal cuts in distance 3D, 5D and 7D from T-junction for inlet concentration 1 mg/m^3 and particle diameter 20 µm for straight supply pipe a), single elbow b) and double elbow supply pipe c). Depicted particles are located in the domain which are in distance from H-0.03 m to H+0.03 m from the T-junction, where H equals 3D, 5D and 7D.

4. Conclusion

The simulation results presented above give qualitative information about distribution of particles in stacks with different geometrical configurations and for different particle diameters. It is shown that the particle diameter has significant influence on the concentration field and depending on the stack design the corresponding measurement uncertainty can be expected. However, for the quantitative assessment of the possible measurement error, the time averaged sum of the particles in sampling points is needed and the corresponding simulated mass flow rate can be calculated as weighted mean with the axial velocity as the weight. By comparison of this emission mass flow rate with its given inlet value, the possible error can be discussed with regard to the number and location of the sampling points as given by the standard EN 15259. This is the aim of the further research.

Acknowledgement

This work was supported through the Joint Research Project 18NRM04 HEROES "*Determining new uncertainty requirements for increasingly stringent legislative HCl industrial emission limits*". This project has received funding from the EMPIR programme co-financed by the Participating States and from the European Union's Horizon 2020 research and innovation programme.

References

[1] E. 1911:2010, „Stationary Source Emissions - Determination of Mass Concentration of Gaseous

Chlorides Expressed as HCl - Standard Reference Method“.

[2] „Best Available Techniques (BAT),“ v *Reference Document on Waste Incineration*, Joint Research Centre, draft 1, May, 2017.

[3] B. EN, „15259:2007 , Air quality Measurement of stationary source emissions Requirements for measurement sections and sites and for measurement objective, plan and report“.

[4] J. Geršl, S. Knotek, Z. Belligoli, R. P. Dwight, R. A. Robinson a M. D. Coleman, „Flow rate measurement in stacks with cyclonic flow - Error estimations using CFD modelling,“ *Measurement*, pp. 167-183, 2018.

[5] S. Knotek, M. Workamp, J. Geršl a M. D. Schakel, „Narrow stack emissions: Error in flow rate measurements due to disturbances and swirl,“ *Journal of the Air & Waste Management Association*, 30 November 2020.

[6] D. M. Snider, „An Incompressible Three-Dimensional Multiphase Particle-in-Cell Model for Dense Particle Flows,“ *Journal of Computational Physics*, pp. 523-549, 1 7 2001.

[7] A. Dehbi, „A CFD model for particle dispersion in turbulent boundary layer flows,“ *Nuclear Engineering and Design (238)*, pp. 707-715, 2008.

[8] B. E. Launder a D. B. Spalding, „The numerical computation of turbulent flows,“ *Comput. Methodfs Appl. Mech. Eng. 3 (2)*, pp. 269-89, 1974.